RESEARCH PAPER

CrossMark

Quantitative analysis of sperm rheotaxis using a microfluidic device

Kari Rappa[1,2] · Jacob Samargia[1] · Mazhar Sher[1,2] · Javier S. Pino[1,2] · Harold F. Rodriguez[3] · Waseem Asghar[1,2,4]

Abstract
Quite puzzling issue in biology is how sperm cells are selected naturally where human sperm has to maintain a correct swimming behavior during the various stages of reproduction process. In nature, sperm has to compete a long journey from cervix to oocyte to stand a chance for fertilization. Although various guidance mechanisms such as chemical and thermal gradients are proposed previously, these mechanisms may only be relevant as sperm reaches very close to the oocyte. Rheotaxis, a phenomenon where sperm cells swim against the flow direction, is possibly the long-range sperm guidance mechanism for successful fertilization. A little is known quantitatively about how flow shear effects may help guide human sperm cells over long distances. Here, we have developed microfluidic devices to quantitatively investigate sperm rheotaxis at various physiological flow conditions. We observed that at certain flow rates sperm actively orient and swim against the flow. Sperm that exhibit positive rheotaxis show better motility and velocity than the control (no-flow condition), however, rheotaxis does not select sperm based on hyaluronic acid (HA) binding potential and morphology. Morphology and HA binding potential may not be a significant factor in sperm transport in natural sperm selection.

Keywords Microfluidics · Sperm selection · Advanced reproductive technology (ART) · In vitro fertilization

1 Introduction

On the journey from ejaculation to fertilization, sperm has to travel a distance that is more than 1000 times than its length (~ 100 μm) to find an oocyte sitting in female's oviduct (Swain et al. 2013; Worrilow et al. 2013). Previously, it was believed that a large number of sperm cells race towards different directions to compete in finding an oocyte. However, with the new scientific knowledge and understanding,

✉ Waseem Asghar
wasghar@fau.edu

1 Asghar-Lab, Micro and Nanotechnology in Medicine, College of Engineering and Computer Science, Boca Raton, FL 33431, USA

2 Department of Computer and Electrical Engineering and Computer Science, Florida Atlantic University, Boca Raton, FL 33431, USA

3 IVF Consultants, Inc., Miramar, FL, USA

4 Department of Biological Sciences, Florida Atlantic University, Boca Raton, FL 33431, USA

it became clear that sperm cells are guided by various mechanisms to guide sperm towards oocyte as reviewed by others and us (Eisenbach and Giojalas 2006; Rappa et al. 2016). In nature, human sperm, ejaculated into the vagina, use active swimming and passive muscular contractions to pass through the uterus and reach the storage site in the isthmus of oviduct. Sperm cells encounter various complex physiological environments including muscular contractions, biochemicals, ciliary currents, and oviductal fluid flow in a direction opposite to the way sperm cells need to go. Various guidance mechanisms such as chemotaxis (sperm movement towards chemoattractant) (Eisenbach and Giojalas 2006; Xie et al. 2010) and thermotaxis (sperm movement due to temperature gradient) (Boryshpolets et al. 2015; Pérez-Cerezales et al. 2015a, b) are proposed, however, muscular contractions and fluid flow would disrupt these gradients over long distances; these mechanisms may only be relevant as sperm reaches very close to an oocyte (Miki and Clapham 2013). Specifically, sexual stimulation of a female increases oviductal discharge, to wash away viscous mucus and globular cells to clear the way for incoming sperm cells (Krüger et al. 2002; Parker 1931). Muscle contraction and ciliary currents help push oviductal discharge to uterus, and sperm cells have to swim against this flow to stand a chance to

fertilize an oocyte. Rheotaxis, a phenomenon where sperm cells swim against the flow direction is possibly the long-range sperm guidance mechanism for successful fertilization (El-sherry et al. 2017; Ishikawa et al. 2016; Mathijssen et al. 2016; Zhang et al. 2016).

Experiments on marine snail (red abalone) that fertilizes externally show that shear flow could have acted as a selective pressure, which is beneficial in the reproduction of these organisms (Riffell and Zimmer 2007; Zimmer and Riffell 2011). In higher organisms, like humans that fertilize internally, the sperm guidance is much more complex due to the cilia-directed flow and muscular contractions which indicate the importance of shear flow in sperm guidance, however, it is difficult to perform well-controlled in vivo experiments in animal models. It is known that similar to algae and bacteria (Chengala et al. 2013; Fu et al. 2012), human sperm are capable to swim against the flow, but this rheotaxis guidance needs further investigation. Although, we know that sperm cells show rheotaxis (Eisenbach and Giojalas 2006; Gaffney et al. 2011; Gillies et al. 2009; Kantsler et al. 2014; Miki and Clapham 2013; Pérez-Cerezales et al. 2015b; Tung et al. 2014) and swim against the flow direction, little is known about optimal flow rates that human sperm cells respond to. Currently, it is unknown whether the sperm cells showing rheotaxis have better functional parameters (motility, velocities, maturity, and morphology) that would help in the selection of high quality sperm for in vitro fertilization, mimicking natural sperm selection. Herein, we develop microfluidic devices to quantitatively investigate the effect of flow on sperm guidance and if this guidance has any role in the selection of high quality sperm.

2 Experimental

2.1 Device fabrication

To study the effect of fluid flow on sperm guidance, we have developed a microfluidic device (Fig. 1a). The design for the device was created in AutoCAD 2015 and uploaded to the UCP Software for cutting the device. The poly-(methyl methacrylate) (PMMA) (McMaster-Carr, Atlanta, GA and ePlastics, San Diego, CA 1.5 and 3 mm thick) and the double sided adhesive (DSA) (3M, St. Paul, MN, 76 μm thick) were cut using a VLS 2.30 laser cutter (VersaLaser, Scottsdale, AZ). The differential fluid flow chip (Fig. 1a) consisted of 1.5 mm PMMA cut into a 28.5 mm×8 mm piece. A 4 mm diameter sperm inlet was cut into the piece 28.5 mm away from a 0.764 mm fluid flow inlet. This was then attached to a piece of DSA which had a 4 mm diameter sperm inlet and a 22.4 mm×4 mm channel cut into it. The whole structure was then attached to a 75 mm×25 mm glass slide (Fig. 1a).

The constant fluid flow and sperm collection chip (Fig. 1b) was made with 3 mm thick PMMA cut into 75 mm×25 mm. A sperm inlet of 4 mm diameter was cut 8 mm away from an elliptical sperm collection chamber (long axis 6 mm, short axis 2.4 mm). The fluid flow inlet with diameter 1.98 mm was cut 13 mm away from the sperm inlet. This piece of PMMA was then attached to a piece of 76 μm DSA with same dimensions of PMMA and a 13 mm×2 mm long channel from flow inlet to sperm inlet (8 mm from elliptical collection chamber to sperm inlet). Three pieces of 3 mm thick PMMA were then cut into dimensions of 10.6 mm×75 mm with a 4 mm diameter sperm inlet. These three pieces were attached by 76 μm DSA

Fig. 1 **a** Differential fluid flow chip consists of 4 mm diameters sperm inlet, 76 μm channel height, and 28.5 mm microchannel length. **b** Constant fluid flow and sperm collection chip consists of 4 mm diameter sperm inlet, 6 mm by 2.5 mm elliptical collection chamber, 76 μm high and 8 mm long microfluidic channel. Images in **a, b** are taken by MS
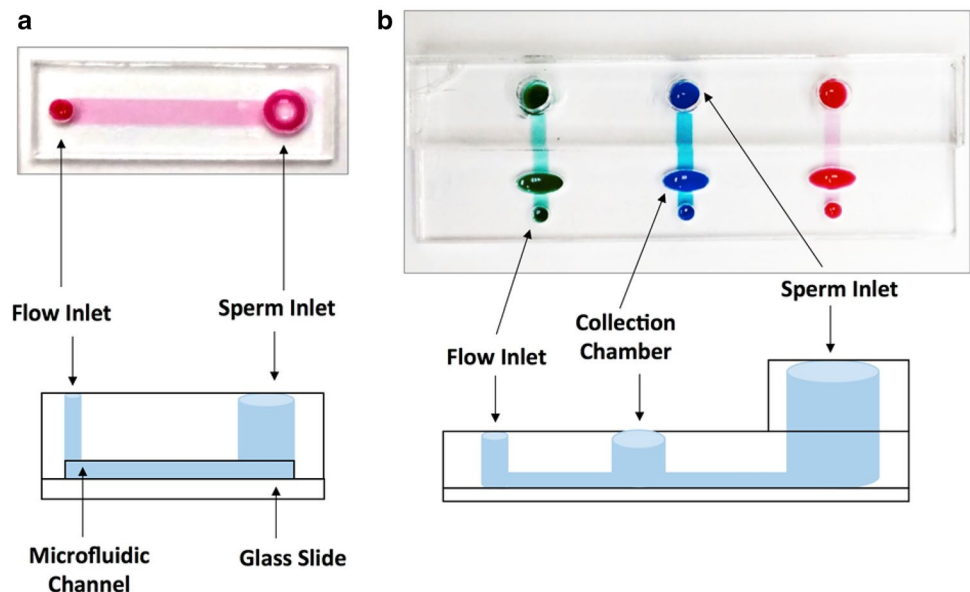
and stacked on top of the sperm inlet of the bottom PMMA piece (Fig. 1b).

2.2 Sperm preparation

Human sperm in 1 mL vials and 0.5 mL canes were purchased from California Cryobank, Fairfax, VA and Cryos International, Orlando, FL and stored in liquid nitrogen. All semen samples were de-identified and anonymous. All methods were carried out in accordance with relevant guidelines and regulations by Institutional Biosafety Committee. Sperm was thawed at 37 °C water bath for 15 min before use.

2.3 Sperm response to flow

HTF-HEPES (InVitroCare, Frederick, MD) buffer supplemented with 1% BSA (FisherSci, Fair Lawn, NJ) was filled into a 10 mL syringe (Becton, Dickson and Company, Franklin Lake, NJ). A 17 gauge blunt needle (SAI, Lake Villa, IL) attached to 0.90″ OD tubing (Cole-Parmer, Vernon Hills, IL) was attached to the syringe. The syringe was then placed on the syringe pump (New Era Pump Systems, East Farmingdale, NY) and pumped in fluid until the channel was filled with HTF-HEPES buffer. The pump was then stopped and allowed to reach an equilibrium state where no flow occurred. A 4 μL sample of semen was then loaded into the sperm inlet of the differential flow chip. The sperm were allowed to swim with no flow for a period of 10 min to allow an ample amount of sperm into the channel. At that point, the syringe pump was turned on at a flow rate of 2, 4, 5, 6, 8 and 10 μL/min. The amount of sperm that oriented and swam against the flow was recorded and manually counted. The sperm motion videos were recorded using a microscope camera at 30 frames per second (fps) before and after flow conditions. Sperm tracks were analyzed using ImageJ (http://rsbweb.nih.gov/ij/) CASA plugin. Rheotaxis was defined as sperm head angle within $\pm 22.5°$ of flow direction or the horizontal image axis.

A constant rate of 3 μL/min was used to sort sperm in the constant flow collection chip (Fig. 1b). The collection chamber was filled with 1% HTF-BSA and then covered with DSA. The syringe pump was turned on and to fill the collection chip was with 1% HTF-BSA. A 10 μL stock sample of semen was loaded into the 4 mm diameter by 15 mm high sperm inlet of the constant flow collection chip. The control group used the similar chip under the same conditions minus the flow. The chips were then left to incubate for an hour before collecting sperm from the collection chamber.

2.4 Sperm concentration

Sperm from the stock, control, and flow experimental groups were counted using Makler chamber (Sefi Medical, Israel) as

per the instructions and labeled as motile, non-progressively motile, or immotile. Each count was taken at least twice and the average of that count used as data point.

2.5 Sperm velocity analysis

The differential fluid flow chip was placed on a light microscope stage and recorded using IC Capture software (The Imaging Source, Charlotte, NC) at a location 5 mm away from the sperm inlet before and after flow for 1 min at 30 fps.

The sperm collected from the constant flow chip was prepared as per WHO guidelines (World Health Organization Laboratory Manual for the Examination and Processing of Human Semen 2010). A 11 μL of sample was placed on a glass slide and covered with a 24 mm×24 mm to give a depth of approximately 20 μL. The sperm swimming tracks were recorded using a Nikon DS-Fi3 camera with NIS-Elements software (Nikon) attached to a light microscope for 1 min at 25 fps. The videos were then uploaded to ImageJ (National Institute of Health) and analyzed using the CASA plugin to obtain the curvilinear velocity (VCL), average path velocity (VAP) and the straight-line velocity (VSL) as previously demonstrated (Asghar et al. 2014b).

2.6 Sperm morphology assessment

Sperm were recovered from the constant flow chip after 1 h. A 2 μL samples from the stock, control, and flow groups were placed on a pre-stained GoldCyto SB sperm blue slide (Fertility Stuff, Murphy, NC) and covered with a 24 mm×24 mm coverslip. The slide was then heated at 60 °C for at least 5 min. The sperm were examined at 1000× and checked for normal or abnormal morphology as per Strict Morphology Criteria (Asghar et al. 2014b); (head must be smooth, regularly contoured, oval, 40–70% acrosomal region, no large vacuoles, no more than two vacuoles; midpiece must be slender, regular, same length as head, major axis aligned with the head, not larger than one-third size of the head; principal piece must have a uniform diameter, thinner than midpiece, approximately 45 μm long, no sharp angles). Atleast 100 sperm were analyzed for 3 times for morphology assessment.

2.7 Hyaluronic acid assay (HBA) binding analysis

Hyaluronic acid binding is a test of sperm maturity with intact acrosome. The cells surrounding the egg, the cumulus oophorous, are surrounded by a hyaluronic gel matrix. Only mature sperm cells are able to penetrate this matrix to get to the egg, hence HA binding is a good indicator of sperm function and maturity (Gaffney et al. 2011; Huszar et al. 2003, 2006, 2007). Sperm were recovered from the constant flow chip after 1 h. A 10 μL sample was placed on

the HBA slide (CELL-VU, New York, NY) and incubated for 30 min as per protocol. Sperm attached and unattached to HBA slide were counted. Each experiment was repeated three times. The number of attached sperm was divided by the total number of sperm counted (attached + unattached) to get the percent sperm that were attached.

2.8 Statistical analysis

Statistical analysis was performed using one-way analysis of variance (ANOVA) for all three groups, and a two-tailed t test assuming unequal variance was used for between two groups. A p value of less than 0.05 was considered statistically significant.

3 Results

3.1 Computational analysis

COMSOL simulations were performed to determine the effects of shear stress on sperm cells in the proposed microfluidic device. A single sperm was modeled as an oval shaped structure with length 5 μm and width 4 μm (World Health Organization Laboratory Manual for the Examination and Processing of Human Semen 2010). A microfluidic channel with a length of 28 mm and height of 76 μm was modeled and a laminar flow conditions were assumed. The no slip boundary conditions were applied to the walls of the microfluidic channel. Various flow rates resulted in different average velocities. A boundary condition with zero pressure was assumed for the outlet (Cheung et al. 2009; Javanmard et al. 2010; Wan et al. 2011). The Navier–Stokes equations were used to simulate the motion of fluid passing by the sperm. Different sizes of meshes were applied

to solve the simulation and velocity and pressure profiles were calculated. The velocity magnitude and streamlines are shown in Fig. 2a, b, respectively. The shear stress was calculated at various flow rates (2, 4, 5, 6, 8, 10, 12 μL/min) and the resultant drag force was determined (Fig. 2c). It was observed that the higher flow rates resulted in increased drag force that impedes the forward movement of sperm against the flow.

3.2 Quantitative sperm response to various flow conditions

We investigated the effect of various flow conditions on sperm rheotaxis using differential flow microfluidic chip (Fig. 1a). Sperm tracking videos were recorded in a microfluidic channel at before and after flow conditions. Sperm tracks and swimming directions were analyzed to determine the number of sperm that oriented and swam against the direction of flow at various flow rates (2, 4, 5, 6, 8 and 10 μL/min). Before the start of flow, sperm cells were moving randomly in all directions (Fig. 3a, e). After flow, the sperm cells oriented against the direction of flow (Fig. 3b, f, Supplementary video S1 and S2). The percentage of sperm that orient their head and actively swim against the flow direction increases from 2 μL/min (61.85 ± 7.08%) to 4 μL/min (67.14 ± 9.63%) before steadily decreasing for the 5 μL/min (41.58 ± 15.28%), 6 μL/min (26.39 ± 7.59%), 8 μL/min (21.04 ± 6.89%), and 10 μL/min flow rates (10.95 ± 9.32%) (Fig. 3c). A one-way ANOVA showed these results to be significantly different across all groups ($p < 0.05$). We observed that at higher flow rate (10 μL/min and higher), almost all the sperm cells were unable to swim forward against the flow due to higher shear flow conditions (Supplementary video S3).
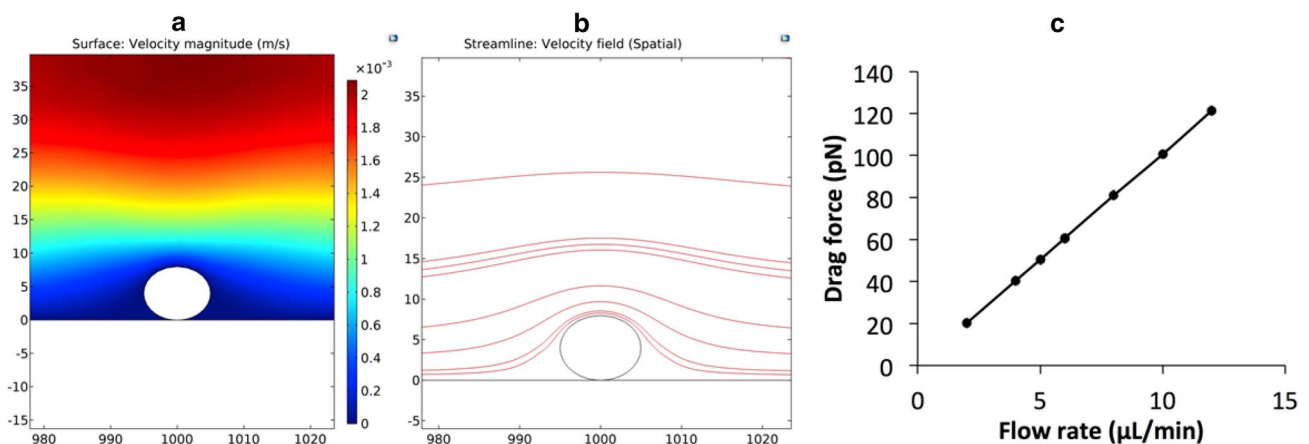

Fig. 2 **a** Simulated flow velocity representation inside a microfluidic device. **b** Streamlines for the velocity field. **c** Graphical representation of the relationship between various flow rates and drag force applied to the sperm inside a microfluidic channel
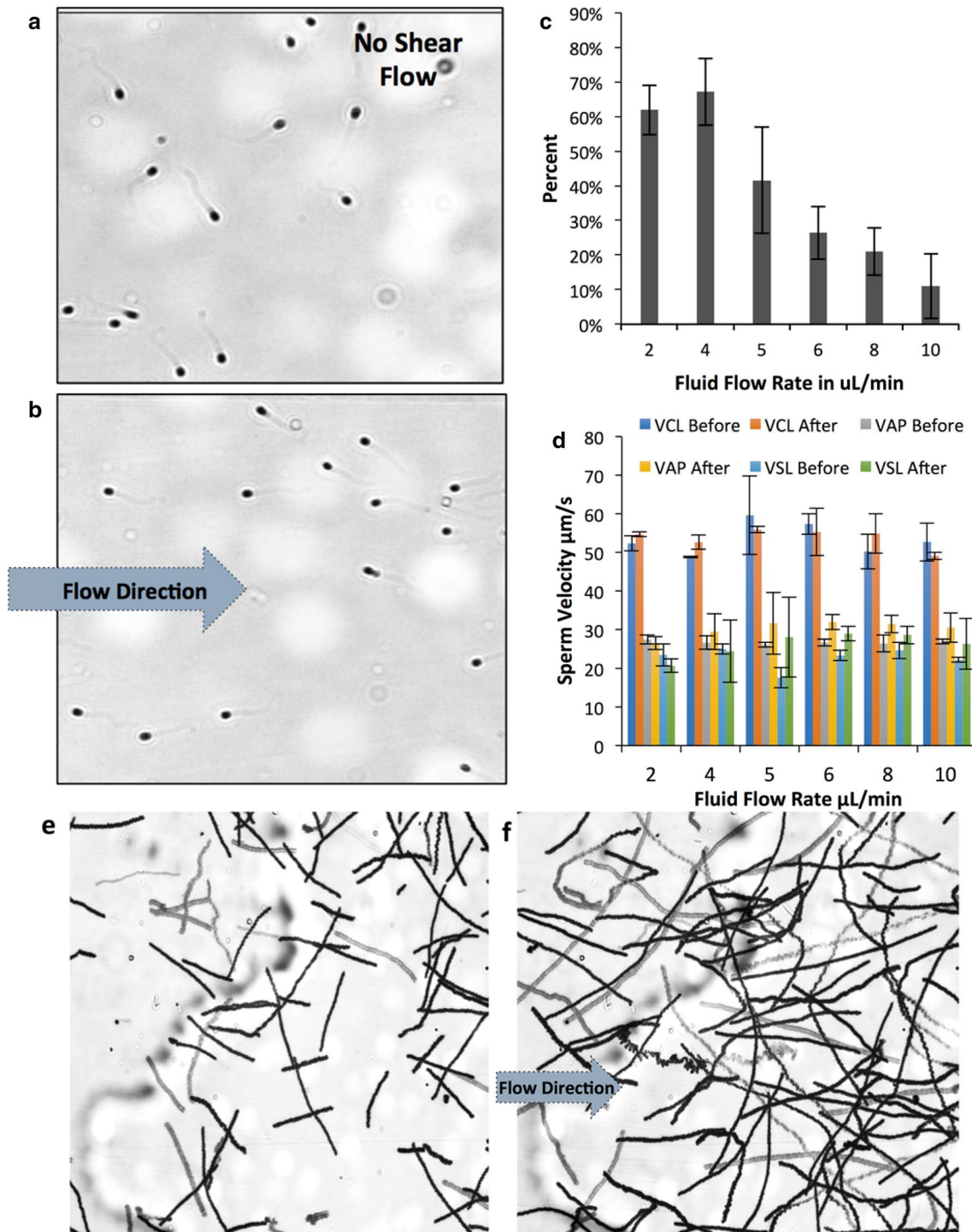
Fig. 3 **a** Sperm position before flow in the differential fluid flow device. **b** Sperm orient and swim in a direction opposite to flow. **c** Percentage of sperm at different flow rate that oriented and progressively swam against flow. Data are shown as average ± standard deviation. $n = 20–200$, $N = 3$. n: number of sperm, N: number of experiments. **d** Curvilinear velocity (VCL), average path velocity (VAP), and straight-line velocity (VSL) before and after flow in the differential fluid flow chip. **e** Sperm paths before flow. **f** Sperm paths during flow. Flow is from left to right

Sperm motility parameters; curvilinear velocity (VCL), average path velocity (VAP) and straight-line velocity (VSL) were measured at before and after flow conditions. The sperm are tracked and their paths at before and after flow conditions were generated by the CASA plugin as seen in Fig. 3e, f respectively. These sperm paths show the random

linear progression of sperm that is normally exhibited in the absence of flow (Fig. 3e). The paths that are curved are a result of a sperm with its head facing downstream turning to head upstream (Fig. 3f). The squiggly paths are from sperm that were trying to swim but are being pushed back by the flow. We observe no significant difference in VCL, VAP and VSL between the six flow rates at before and after flow conditions ($p > 0.05$) (Fig. 3d, Supplementary Table 1a, 1b).

3.3 Sperm showing rheotaxis have higher progressive motility

Concentration of sperm in million sperm/mL and type of motility was calculated in each experimental group; (PR) progressive motility, (NP) non-progressive motility, (IM) immotility, and (PR + NP) total motility (Fig. 4a). The total stock sperm (unsorted raw sperm sample) concentration ($59 \pm 17 \times 10^6$/mL) is significantly larger than both the control (no flow-condition) ($7.0 \pm 9.0 \times 10^6$/mL) and

flow ($11 \pm 6 \times 10^6$/mL) concentrations ($p < 0.05$). The stock concentration also has a significantly larger concentration of PR ($17 \pm 12 \times 10^6$/mL), NP ($6.5 \pm 3 \times 10^6$/mL), IM ($36 \pm 11 \times 10^6$/mL) and total motile ($23 \pm 14 \times 10^6$/mL) than the control and flow groups ($p < 0.05$). The flow and control groups show no significant difference between their total concentration of sperm recovered after sorting ($p > 0.05$), however, the flow group does have a higher concentration of PR sperm ($8.6 \pm 4.5 \times 10^6$/mL) and total motile sperm (9.6 ± 5.210^6/mL) than the no-flow control (3.3 ± 3 and $5.2 \pm 5.7 \times 10^6$/mL, respectively) (Fig. 4a).

Sperm motility was assessed based upon motile, non-progressively motile and immotile. The average percentage of motile sperm for stock, control, and flow experimental group is 27.66 ± 11.43, 46.85 ± 36.60 and $82.98 \pm 15.06\%$, respectively (Fig. 4b). The percent of motile sperm found in the flow group is significantly higher than that found in stock group ($p < 0.05$). The total sperm motility (M + NP) in flow group was significantly higher ($91.02 \pm 9.49\%$) than stock
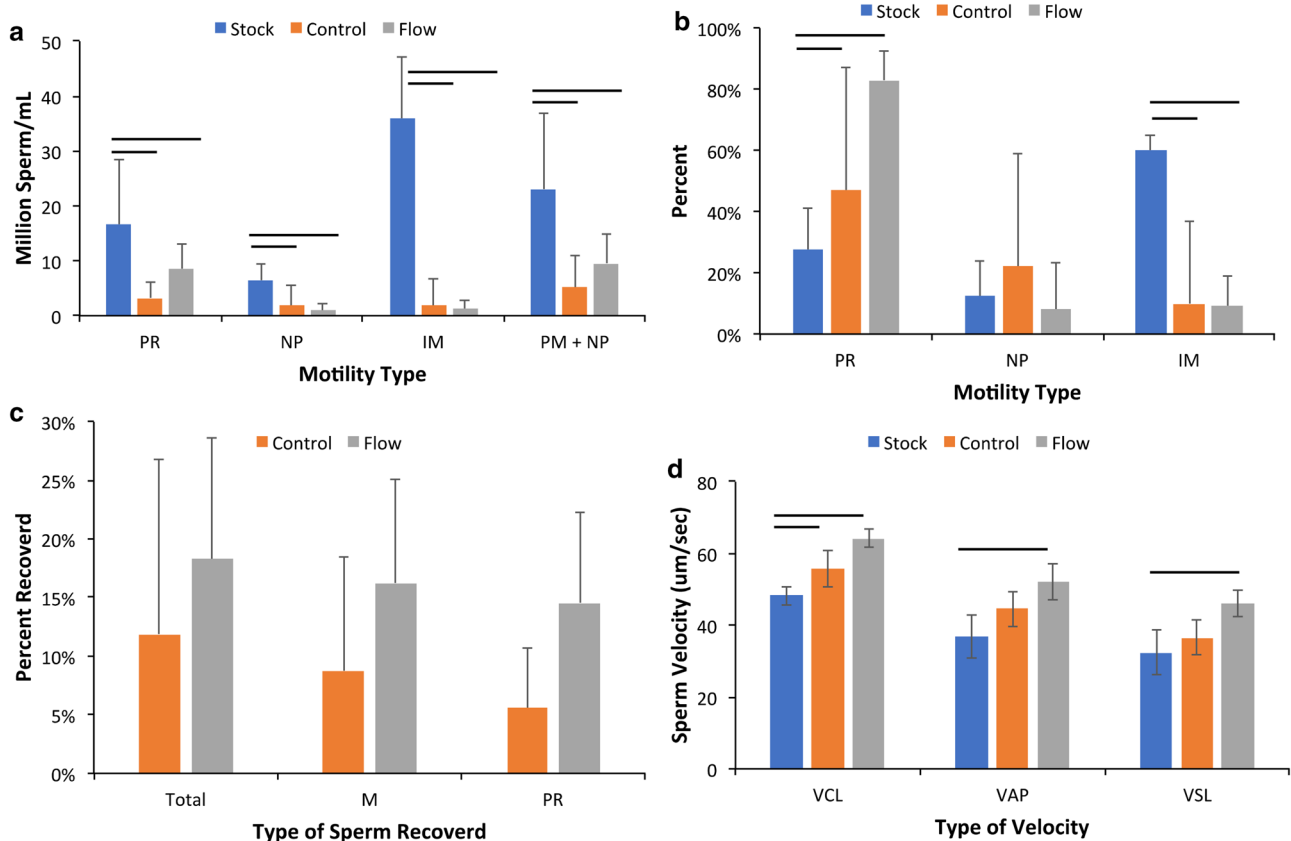

Fig. 4 **a** Concentration of sperm in million sperm/mL and type of motility observed in each experimental group; (PR) progressive motility, (NP) non-progressive motility, (IM) immotility, and (PR + NP) total motility. **b** Motility type of sperm recovered from constant fluid flow collection chip; (PR) progressive motility, (NP) non-progressive motility, and (IM) immotility. **c** Percent of sperm recovered from the collection chip after 1 h; (M) motility includ-

ing non-progressive motility, and (PR) progressive motility. **d** Sperm VCL, VAP, and VSL for stock (raw semen sample), control, and flow sorted sperm. Flow rate used for all these results was 3 μL/min. Data are shown as average ± standard deviation. The statistical significance between samples is marked with a straight line on the top of the graphs (p value < 0.05)

$(40.17 \pm 13.68\%)$ ($p < 0.05$). The average percent of immotile sperm for stock, control and flow groups were 59.83 ± 13.68, 9.95 ± 17.86, and $8.98 \pm 9.49\%$, respectively. The stock has a significantly higher amount of immotile sperm compared to both the control and flow groups ($p < 0.05$) (Fig. 4b).

The percent of sperm recovered from the control and flow group is 11.88 ± 14.94 and $18.26 \pm 10.31\%$. The flow group has a larger recovery of motile ($16.24 \pm 8.78\%$) and progressively motile ($14.54 \pm 7.66\%$) sperm as compared to the control, whose values are 8.75 ± 9.75 and $5.54 \pm 5.09\%$, respectively (Fig. 4c), however difference is statistically insignificant.

3.4 Sperm showing rheotaxis have higher sperm velocity parameters

To determine the sperm swimming speed and linearity, the sperm kinematics need to be known. Supplementary table 2 shows the average kinematics of the stock, control, and flow groups. Sperm sorted in flow group show significantly higher values in VCL, VAP, VSL than the control and stock (Fig. 4d). The control VCL is also significantly larger than the stock. There is no significant difference between the linearity (describes path curvature) or the wobble (how many times the head crosses over the VAP).

3.5 Rheotaxis does not select sperm based on hyaluronic acid (HA) binding and morphology

The percent of sperm that bound to the hyaluronic acid is 83.9 ± 6, 89.3 ± 15 and $90.7 \pm 6\%$ for the stock, control and flow groups, respectively (Fig. 5a). There is an increase in the amount of sperm that bind in the control and flow groups, but the difference is not significant ($p < 0.05$).

The average values for the percent of the sperm sample that are morphologically normal is 5.11 ± 1.26, 4.25 ± 3.81 and $5.48 \pm 3.40\%$ for the stock, control and flow groups, respectively (Fig. 5b). We observe no significant difference in normal sperm morphology in all three experimental groups (stock, control, and flow).

4 Discussion

Infertility affects roughly 48.5 million couples worldwide and 30–50% of these cases are caused by male factor infertility (Boivin et al. 2007; Dyer 2009; Mascarenhas et al. 2012; Ombelet et al. 2008). Assisted reproductive technologies (ART), such as intracytoplasmic sperm injection (ICSI), intrauterine insemination (IUI) and in vitro fertilization (IVF) offer infertile couples the opportunity to start families. However, only about a third of ART cycles result in a
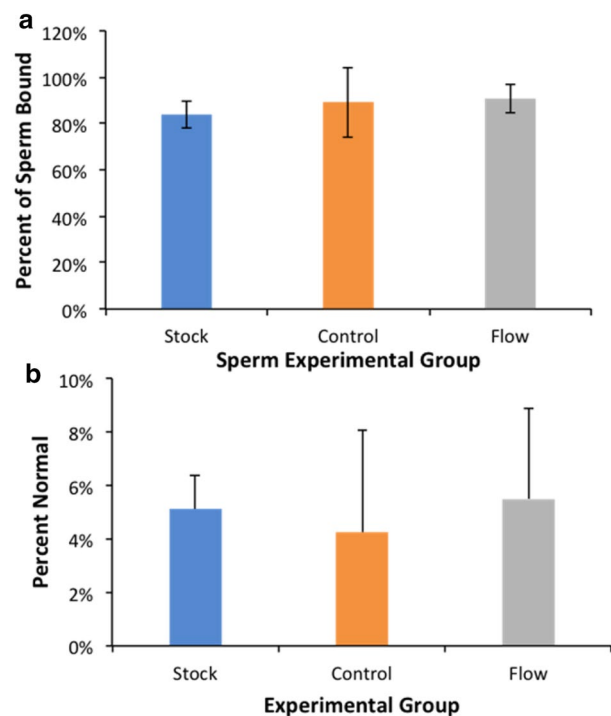
Fig. 5 a Percent of sperm in stock, control, and flow (4 μL/min) that bound to hyaluronic acid. **b** Percent of sperm having normal morphology in stock, control, and flow (3 μL/min) sorted sperm. Data are shown as average ± standard deviation. $n = 100$–200, $N = 3$. n: number of sperm, N: number of experiments

birth (Rappa et al. 2016). Sperm processing is an important part of the ART cycle and there are several factors to consider when determining the quality of sperm, such as sperm concentration, motility, morphology, DNA integrity and levels of reactive oxygen species (ROS). Infertile men tend to have abnormal sperm parameters, such as low concentration, abnormal morphology and elevated levels of DNA damage and ROS (Asghar et al. 2014b; Larson-Cook et al. 2003; Pasqualotto et al. 2000).

The most frequently used methods of sperm sorting and processing including sperm washing, direct swim-up (DSW) and discontinuous density gradient centrifugation (DGC) involve multiple centrifugation steps that are damaging to sperm cells (Asghar et al. 2014b; Nosrati et al. 2014; Rappa et al. 2016). Centrifugation creates a sperm pellet that can also include inflammatory cells and immature sperm, which produce ROS and can cause DNA fragmentation in the healthy sperm cells (Aitken et al. 2013a, b; González-Marín et al. 2012). In natural reproduction, a successful pregnancy occurs when sperm travel through the female genital tract and fertilize the oocyte in the oviduct. Only about one sperm per every million sperm ejaculated makes it to the oviduct (Eisenbach and Giojalas 2006). The small amount of sperm that are capable of fertilizing the

oocyte indicates that natural sperm selection has a stringent sperm selection process that incorporates muscular contractions and significant fluid flow against the sperm swimming direction. Centrifugation is not involved in natural sperm selection in female genital track, hence current lab-based sperm sorting methods produce unknown bias and damage sperm cells. Hence, it is important to continue to search for way to improve sperm processing and sorting procedures to create the best pregnancy outcomes.

Microfluidics has emerged as an alternative technology with precise control to sort and isolate cells within small volumes. Microfluidics has been widely investigated for various applications in cell sorting, disease diagnostics and regenerative medicine (Asghar et al. 2014a; Coarsey et al. 2017; Kanakasabapathy et al. 2017; Sharma et al. 2018; Yu et al. 2018). More recently, microfluidic based devices have been reported to sort and select healthy sperm to be utilized in ART procedures (Knowlton et al. 2015; Rappa et al. 2016). Microfluidic technology provides precise control to optimize the microchannel dimensions and surface topography such that motile sperm cells are enriched after sorting (Chinnasamy et al. 2018; Tung et al. 2014). Using microfluidic technology, sperm are either sorted based on their passive motility or microfluidic based sorting is integrated with sperm guidance mechanisms such as chemotaxis and thermotaxis (Knowlton et al. 2015; Rappa et al. 2016). More recently, flow-driven microfluidic devices are also developed (Chen et al. 2011, 2013; Cho et al. 2003; Seo et al. 2007) where motile sperm cells either flow with or against the flow during the sorting process, however, these microfluidic devices are not utilized in clinical practice and requires further investigation. Its not clear in the literature that whether microfluidic based sperm sorting provides any quantifiable advantage over other technologies in terms of sperm functional parameters including sperm velocity and HA binding. A good sperm processing technique will be able to select normal sperm mimicking natural sperm selection, while eliminating the damaging centrifugation steps and remove harmful substances such as dead cells and ROS producing leukocytes that can cause damage. Sperm rheotaxis is believed to be the possible long-range sperm guidance mechanism in natural sperm selection (El-sherry et al. 2017; Ishikawa et al. 2016; Mathijssen et al. 2016; Zhang et al. 2016). We have developed microfluidic devices to quantitatively investigate the effect of fluid flow on human sperm guidance and selection.

The flow rate of human oviductal fluid is not known (Miki and Clapham 2013; Tung et al. 2014), therefore, we analyzed sperm rheotaxis at various flow rates to find out the optimal shear flow where maximum number of sperm cells show rheotaxis. From sperm rheotaxis experiments, the best flow rate determined using the differential fluid flow chip was observed to be 2–4 µL/min where $61.85 \pm 7.08\%$ (2 µL/min,

20.2 pN drag force) to $67.14 \pm 9.63\%$ (4 µL/min, 40.4 pN drag force) of sperm show rheotaxis (Figs. 2c, 3c).

The paths of the sperm before flow follow a relatively straight curvilinear path (Fig. 3e). After flow, the sperm that were already swimming upstream continue to do so. Sperm cells whose heads were facing downstream from flow direction made in arc like trajectory to turn themselves to face into the flow (Fig. 3f). This shows the sperm are responding to the flow near a surface with a chiral flagellar pattern. The sperm tail is in a spot of higher shear flow than the head is at a surface, thus, the hydrodynamic forces and steric repulsion help turn the sperm to face upstream (Ishimoto and Gaffney 2015; Kantsler et al. 2014). In parabolic flow condition as in the case of microfluidic channel where there is maximum flow towards the middle of the channel and almost zero flow at the boundary, sperm long tail is subjected to more force in high flow gradient compared to sperm head pointing towards the wall boundary where there is minimal force due to flow. These differential forces on sperm tail and head result into the tail being dragged downstream with the head pointed upstream (Bretherton 1961). As the fluid flow rate is increased above 6 µL/min, the majority of the sperm were being swept away. There was no significant difference between the sperm kinematics before and after flow when sperm cells were tracked while keeping the flow on (Fig. 3d). This is most likely due to the sperm being able to actively swim against the flow, but the flow impeding some forward progress.

We observe that the control (no-flow) and flow groups have similar total concentration of sorted sperm (PM + NP), but the flow has a higher concentration of progressively motile sperm (Fig. 4a). This can be explained because the flow would select for more progressively motile and healthier sperm than a no-flow condition, which would allow for sperm with erratic swimming patterns to still traverse the channel. Both the control and flow groups contained some non-progressively motile sperm. It is possible that a small space between input and collection chamber in the device leads to contamination of dead and/or non-progressively motile sperm cells, and that increasing the distance between input and collection chambers of the device can prevent contamination due to non-progressive and dead sperm.

Sperm kinematics need to be analyzed before and after collection to understand how flow affects sperm sorting process and aid in selecting healthy sperm with better velocity, swimming behavior and motility. The sperm that were analyzed after collection were limited to a 20 µm deep chamber that effectively kept them in the *xy*-plane (Cooper et al. 2010). The flow group had velocities significantly higher than stock group (Fig. 4d). An increase in velocity is expected because only fast sperm will be able to travel the length of the channel against stream. The increase of velocity in the control group (VCL only) over the stock group is

also expected because sperm that travel down microfluidic channels have higher velocities than the stock semen sample (Asghar et al. 2014b; Tasoglu et al. 2013). From these results its clear that rheotaxis aids in selecting high quality sperm with higher velocity parameters. Supplementary videos S1 and S2 support the conclusion where mostly highly motile sperm cells are able to progress forward against the flow and small headed immature sperm cells with broken mid piece are not able to swim against the flow. Supplementary video S4 shows the sperm rheotaxis at higher magnification and also supports the conclusion that only most motile sperm cells can progress forward against the flow.

To further investigate the functional parameters of sorted sperm, sperm were analyzed for HA binding and morphology. We observe no significant difference between the experimental groups in the percent of sperm that bound to HA coated slides, suggesting that rheotaxis does not depend on sperm's ability to bind with HA (Fig. 5a). This also goes along with the finding that rheotaxis is most likely a passive and physical process (Ishimoto and Gaffney 2015; Kantsler et al. 2014; Zhang et al. 2016). Although HA binding shows sperm maturity, sperm showing HA binding does not improve clinical outcome in terms of fertilization rates and clinical pregnancy. (Beck-Fruchter et al. 2016; Ghaleno et al. 2016; Kovacs et al. 2011; Tarozzi et al. 2009).

The three experimental groups (flow, no-flow, stock) do not show any statistically significant difference between morphologically normal sperm. Fluid flow does not appear to be able to select sperm based on morphology. Although sperm morphology is currently used to assess the quality of sperm sample, the value morphology has on determining quality of sperm has been recently called into question as the data collected is dependent on the laboratory doing the test, morphology assessment lacking analytical reliability, and subjective nature of morphological assessment (Gatimel et al. 2017). Another study argued that sperm morphology was of little clinical value, showing that men with a complete absence of normal sperm morphology exhibited high rates of spontaneous pregnancy (Kovac et al. 2017). In our case, morphology analysis results indicates that rheotaxis based sperm sorting does not select sperm based on sperm morphology, which may be the case in natural sperm selection as morphology or the way morphology is assessed is found to have little clinical value.

5 Conclusions

In natural sperm selection, sperm has to travel a long distance against fluid flow before standing a chance for fertilization. To quantitatively investigate the effect of fluid flow on sperm guidance in vitro, we have developed microfluidic devices and found that the optimal flow rate to sort sperm based on rheotaxis is 2–4 μL/min (20.2–40.4 pN drag force) as more than 60% sperm show rheotaxis at such flow conditions. Sperm sorted using constant fluid flow chip (at flow rate of 3 μL/min, 30.3 pN drag force) show significantly higher motility characteristics than the stock sample and no-flow sorted sperm. We also observed that rheotaxis does not select human sperm based on HA binding and morphology as both of these parameters are not significanlty changed in sperm sorted using rheotaxis. This microfluidic study offers a new evidence that sperm morphology and HA binding potential may not be a significant factor in sperm transport in natural sperm selection as rheotaxis does not select sperm based on HA binding potential and morphology. Considering the capability of the developed device to handle small semen volumes, the sperm sorting device would be best used for IVF or ICSI rather than IUI. With 40–50% of infertility cases being caused by male infertility, it is important to continue research methods to sort and select healthy sperm based on natural sperm guidance mechanisms, without the risk of damages and defects produced by centrifugation based sorting systems currently used in clinical laboratories. In addition, our results have implications beyond human fertility including biodiversity and conservation of endangered or rare species.

Compliance with ethical standards

Conflict of interest The authors declare no competing interests.

References

Aitken R, Bronson R, Smith T, De Iuliis G (2013a) The source and significance of DNA damage in human spermatozoa; a commentary on diagnostic strategies and straw man fallacies. Mol Hum Reprod 19:475–485

Aitken R et al (2013b) On methods for the detection of reactive oxygen species generation by human spermatozoa: analysis of the cellular responses to catechol oestrogen, lipid aldehyde, menadione and arachidonic acid. Andrology 1:192–205

Asghar W, El Assal R, Shafiee H, Anchan RM, Demirci U (2014a) Preserving human cells for regenerative, reproductive, and transfusion medicine. Biotechnol J 9:895–903

Asghar W et al (2014b) Selection of functional human sperm with higher DNA integrity and fewer reactive oxygen species. Adv Healthc Mater 3:1671–1679

Beck-Fruchter R, Shalev E, Weiss A (2016) Clinical benefit using sperm hyaluronic acid binding technique in ICSI cycles: a systematic review and meta-analysis. Reprod Biomed Online 32:286–298

Boivin J, Bunting L, Collins JA, Nygren KG (2007) International estimates of infertility prevalence and treatment-seeking: potential need and demand for infertility medical care. Hum Reprod 22:1506–1512

Boryshpolets S, Pérez-Cerezales S, Eisenbach M (2015) Behavioral mechanism of human sperm in thermotaxis: a role for hyperactivation. Hum Reprod 30:884–892

Bretherton F (1961) Rheotaxis of spermatozoa. Proc R Soc Lond B Biol Sci 153:490–502

Chen Y-A, Huang Z-W, Tsai F-S, Chen C-Y, Lin C-M, Wo AM (2011) Analysis of sperm concentration and motility in a microfluidic device. Microfluid Nanofluid 10:59–67

Chen C-Y et al (2013) Sperm quality assessment via separation sedimentation in a microfluidic device. Analyst 138:4967–4974

Chengala A, Hondzo M, Sheng J (2013) Microalga propels along vorticity direction in a shear flow. Phys Rev E 87:052704

Cheung LSL et al (2009) Detachment of captured cancer cells under flow acceleration in a bio-functionalized microchannel. Lab Chip 9:1721–1731

Chinnasamy T et al (2018) Guidance and self-sorting of active swimmers: 3D periodic arrays increase persistence length of human sperm selecting for the fittest. Adv Sci 5:1700531

Cho BS, Schuster TG, Zhu X, Chang D, Smith GD, Takayama S (2003) Passively driven integrated microfluidic system for separation of motile sperm. Anal Chem 75:1671–1675

Coarsey CT, Esiobu N, Narayanan R, Pavlovic M, Shafiee H, Asghar W (2017) Strategies in Ebola virus disease (EVD) diagnostics at the point of care. Crit Rev Microbiol 43:779–798

Cooper TG et al (2010) World Health Organization reference values for human semen characteristics. Hum Reprod Update 16:231–245

Dyer S (2009) International estimates on infertility prevalence and treatment seeking: potential need and demand for medical care. Hum Reprod 24:2379–2380

Eisenbach M, Giojalas LC (2006) Sperm guidance in mammals—an unpaved road to the egg. Nat Rev Mol Cell Biol 7:276–285

El-sherry T, Abdel-Ghani M, Abou-Khalil N, Elsayed M, Abdelgawad M (2017) Effect of pH on rheotaxis of bull sperm using microfluidics. Reprod Domest Anim 52:781–790

Fu HC, Powers TR, Stocker R (2012) Bacterial rheotaxis. Proc Natl Acad Sci 109:4780–4785

Gaffney E, Gadêlha H, Smith D, Blake J, Kirkman-Brown J (2011) Mammalian sperm motility: observation and theory. Annu Rev Fluid Mech 43:501–528

Gatimel N, Moreau J, Parinaud J, Léandri R (2017) Sperm morphology: assessment, pathophysiology, clinical relevance, and state of the art in 2017. Andrology 5:845–862

Ghaleno LR, Valojerdi MR, Chehrazi M, Samani FS, Yazdi RS (2016) Hyaluronic acid binding assay is highly sensitive to select human spermatozoa with good progressive motility, morphology, and nuclear maturity. Gynecol Obstet Investig 81:244–250

Gillies EA, Cannon RM, Green RB, Pacey AA (2009) Hydrodynamic propulsion of human sperm. J Fluid Mech 625:445–474

González-Marín C, Gosálvez J, Roy R (2012) Types, causes, detection and repair of DNA fragmentation in animal and human sperm cells. Int J Mol Sci 13:14026–14052

Huszar G, Ozenci CC, Cayli S, Zavaczki Z, Hansch E, Vigue L (2003) Hyaluronic acid binding by human sperm indicates cellular maturity, viability, and unreacted acrosomal status. Fertil Steril 79:1616–1624

Huszar G, Ozkavukcu S, Jakab A, Celik-Ozenci C, Sati GL, Cayli S (2006) Hyaluronic acid binding ability of human sperm reflects cellular maturity and fertilizing potential: selection of sperm for intracytoplasmic sperm injection. Curr Opin Obstet Gynecol 18:260–267

Huszar G, Jakab A, Sakkas D, Ozenci C-C, Cayli S, Delpiano E, Ozkavukcu S (2007) Fertility testing and ICSI sperm selection by hyaluronic acid binding: clinical and genetic aspects. Reprod Biomed Online 14:650–663

Ishikawa Y, Usui T, Yamashita M, Kanemori Y, Baba T (2016) Surfing and swimming of ejaculated sperm in the mouse oviduct 1. Biol Reprod 94:81–89

Ishimoto K, Gaffney EA (2015) Fluid flow and sperm guidance: a simulation study of hydrodynamic sperm rheotaxis. J R Soc Interface 12:20150172

Javanmard M, Babrzadeh F, Davis R (2010) Microfluidic force spectroscopy for characterization of biomolecular interactions with piconewton resolution. Appl Phys Lett 97:173704

Kanakasabapathy MK et al (2017) Rapid, label-free CD4 testing using a smartphone compatible device. Lab Chip 17:2910–2919

Kantsler V, Dunkel J, Blayney M, Goldstein RE (2014) Rheotaxis facilitates upstream navigation of mammalian sperm cells. Elife 3:e02403

Knowlton SM, Sadasivam M, Tasoglu S (2015) Microfluidics for sperm research. Trends Biotechnol 33:221–229

Kovac JR, Smith RP, Cajipe M, Lamb DJ, Lipshultz LI (2017) Men with a complete absence of normal sperm morphology exhibit high rates of success without assisted reproduction. Asian J Androl 19:39

Kovacs P, Kovats T, Sajgo A, Szollosi J, Matyas S, Kaali SG (2011) The role of hyaluronic acid binding assay in choosing the fertilization method for patients undergoing IVF for unexplained infertility. J Assist Reprod Genet 28:49–54

Krüger TH, Haake P, Hartmann U, Schedlowski M, Exton MS (2002) Orgasm-induced prolactin secretion: feedback control of sexual drive? Neurosci Biobehav Rev 26:31–44

Larson-Cook KL, Brannian JD, Hansen KA, Kasperson KM, Aamold ET, Evenson DP (2003) Relationship between the outcomes of assisted reproductive techniques and sperm DNA fragmentation as measured by the sperm chromatin structure assay. Fertil Steril 80:895–902

Mascarenhas MN, Flaxman SR, Boerma T, Vanderpoel S, Stevens GA (2012) National, regional, and global trends in infertility prevalence since 1990: a systematic analysis of 277 health surveys. PLOS Med 9(12):1–12

Mathijssen AJ, Shendruk TN, Yeomans JM, Doostmohammadi A (2016) Upstream swimming in microbiological flows. Phys Rev Lett 116:028104

Miki K, Clapham DE (2013) Rheotaxis guides mammalian sperm. Curr Biol 23:443–452

Nosrati R, Vollmer M, Eamer L, San Gabriel MC, Zeidan K, Zini A, Sinton D (2014) Rapid selection of sperm with high DNA integrity. Lab Chip 14:1142–1150

Ombelet W, Cooke I, Dyer S, Serour G, Devroey P (2008) Infertility and the provision of infertility medical services in developing countries. Hum Reprod Update 14:605–621. https://doi.org/10.1093/humupd/dmn042

Parker GH (1931) The passage of sperms and of eggs through the oviducts in terrestrial vertebrates. Philos Trans R Soc Lond Ser B Contain Pap Biol Character 219:381–419

Pasqualotto FF, Sharma RK, Nelson DR, Thomas AJ Jr, Agarwal A (2000) Relationship between oxidative stress, semen characteristics, and clinical diagnosis in men undergoing infertility investigation. Fertil Steril 73:459–464

Pérez-Cerezales S, Boryshpolets S, Afanzar O, Brandis A, Nevo R, Kiss V, Eisenbach M (2015a) Involvement of opsins in mammalian sperm thermotaxis. Sci Rep 5:16146

Pérez-Cerezales S, Boryshpolets S, Eisenbach M (2015b) Behavioral mechanisms of mammalian sperm guidance. Asian J Androl 17:628

Rappa KL, Rodriguez HF, Hakkarainen GC, Anchan RM, Mutter GL, Asghar W (2016) Sperm processing for advanced reproductive technologies: where are we today? Biotechnol Adv 34:578–587

Riffell JA, Zimmer RK (2007) Sex and flow: the consequences of fluid shear for sperm–egg interactions. J Exp Biol 210:3644–3660

Seo D-b, Agca Y, Feng Z, Critser JK (2007) Development of sorting, aligning, and orienting motile sperm using microfluidic device operated by hydrostatic pressure. Microfluid Nanofluid 3:561–570

Sharma S, Zhuang R, Long M, Pavlovic M, Kang Y, Ilyas A, Asghar W (2018) Circulating tumor cell isolation, culture, and downstream molecular analysis. Biotechnol Adv 36:1063–1078

Swain J, Lai D, Takayama S, Smith G (2013) Thinking big by thinking small: application of microfluidic technology to improve ART. Lab Chip 13:1213–1224

Tarozzi N, Nadalini M, Bizzaro D, Serrao L, Fava L, Scaravelli G, Borini A (2009) Sperm–hyaluronan-binding assay: clinical value in conventional IVF under Italian law. Reprod Biomed Online 19:35–43

Tasoglu S et al (2013) Exhaustion of racing sperm in nature-mimicking microfluidic channels during sorting. Small 9:3374–3384. https://doi.org/10.1002/smll.201300020

Tung C-k, Ardon F, Fiore AG, Suarez SS, Wu M (2014) Cooperative roles of biological flow and surface topography in guiding sperm migration revealed by a microfluidic model. Lab Chip 14:1348–1356

Wan Y, Tan J, Asghar W, Kim Y-t, Liu Y, Iqbal SM (2011) Velocity effect on aptamer-based circulating tumor cell isolation in microfluidic devices. J Phys Chem B 115:13891–13896

World Health Organization (2010) Laboratory manual for the examination and processing of human semen. World Health Organization, Geneva

Worrilow K et al (2013) Use of hyaluronan in the selection of sperm for intracytoplasmic sperm injection (ICSI): significant improvement in clinical outcomes—multicenter, double-blinded and randomized controlled trial. Hum Reprod 28:306–314

Xie L et al (2010) Integration of sperm motility and chemotaxis screening with a microchannel-based device. Clin Chem 56:1270–1278

Yu S, Rubin M, Geevarughese S, Pino J, Rodriguez H, Asghar W (2018) Emerging technologies for home-based semen analysis. Andrology 6:10–19

Zhang Z, Liu J, Meriano J, Ru C, Xie S, Luo J, Sun Y (2016) Human sperm rheotaxis: a passive physical process. Sci Rep 6:23553

Zimmer RK, Riffell JA (2011) Sperm chemotaxis, fluid shear, and the evolution of sexual reproduction. Proc Natl Acad Sci 108:13200–13205